

**Corrosion behavior of ARB process of nanostructured aluminium alloys in contact with phase change materials based on  $\text{Na}_2\text{HPO}_4 \cdot 12\text{H}_2\text{O}$  and  $\text{Zn}(\text{NO}_3)_2 \cdot 6\text{H}_2\text{O}$  molten salts**

Mohammad mahdi Taherian, Mardali Yousefpour<sup>1\*</sup>, Ehsan Borhani

Faculty of Materials and Metallurgical Engineering, Semnan University, Semnan, Iran

**Abstract**

Phase change materials (PCM), have high thermal energy storage, based on the latent heat of melting. Hydrate salts are one of the most used PCM. The low heat flux and the insufficient long term stability of the storage materials and containers are two main problems in the energy storage systems. Therefore, in the present article the second problem was investigated and selected different common metals (Fine-grained Al1100 and Al6061 alloys by the six-passes of accumulative roll bonding (ARB) process), and tested their corrosion resistance in contact with salt hydrates that were used as PCMs ( $\text{Na}_2\text{HPO}_4 \cdot 12\text{H}_2\text{O}$  and  $\text{Zn}(\text{NO}_3)_2 \cdot 6\text{H}_2\text{O}$ ). The used method was immersion test. For this purpose, samples were placed in test tubes containing molten hydrate salts into thermo-static water bath in three different time periods of six, twelve and eighteen days in the 55 to 60 °C temperature range. After each period, the rate of weight loss of samples was measured and then the corrosion rate was calculated. The corrosion rate of the ARB processed Al 1100 and Al 6061 alloys in the  $\text{Na}_2\text{HPO}_4 \cdot 12\text{H}_2\text{O}$  at the end of the eighteen days obtained 103.07 and 78.82 mpy, respectively. Also the corrosion rate of ARB Al 1100 Al6061 alloys in the  $\text{Zn}(\text{NO}_3)_2 \cdot 6\text{H}_2\text{O}$  at the end of eighteen days, was obtained 88.67 and 68.71 mpy, respectively. The results show that, in the molten  $\text{Na}_2\text{HPO}_4 \cdot 12\text{H}_2\text{O}$ , the corrosion rate of the

1\*: Faculty of Materials and Metallurgical Engineering, Semnan University, Semnan, Iran, Tel: +982333383385, Fax:+982333654119

E-mail address1: [myousefpor@semnan.ac.ir](mailto:myousefpor@semnan.ac.ir)

E-mail address2: [mardaliyousefpour@yahoo.com](mailto:mardaliyousefpour@yahoo.com)

ARB processed Al1100 alloy is less than ARBed Al6061 alloy, while the corrosion rate for the ARB processed Al6061 alloy in the molten Zn(NO<sub>3</sub>) 2.6H<sub>2</sub>O, is less than ARBed Al1100 alloy.

**Key words:** Aluminium alloy, Phase change materials (PCM), Accumulative Roll Bonding (ARB) process, corrosion rate, corrosion resistance

## 1. Introduction

Nowadays, there are a variety of methods for storing of thermal energy in order to reduce its consumption and availability in needed time. The latent heat is known as one of the most important methods of thermal energy storage. In the latent heat storage methods, when there is small changes in temperature between the temperature of the energy storage and its release, density energy is more than sensible heat storage methods [1, 2]. Storage of latent heat through the phase changing of solid - solid, solid - liquid, liquid - gas and solid - gas are done. Virtually the phase changing of solid to gas or liquid to gas can not be a good source for latent energy storage, since duration the phase conversion, large volume changes, and various boundary conditions are happened. Therefore, the phase changing of solid - liquid and solid - solid provide a good condition for storing of the energy [3]. Phase change materials can store latent energy by phase changing. There are a variety phase change materials with different applications that can be noted organic compounds such as fatty acids, paraffin, and inorganic compounds such as salts and hydrates. Today, many improvements in solar collector systems for energy storage have been done by PCM's [4, 5]. They have recently been employed for applications of solar cooling (cooling solar) and refrigeration and results have been published [6]. Also, solar panels coupled with PMC improve the performance of the panels in comparison with when there are no PCM. So that the solar panels coupled with PCM under the same temperature and the same solar constant, keep their performance in more time, in contrast to solar panels without PCM [7]. Phase change

materials have wide application for energy storage, in construction and related industries [8].

Hydrate salt is one of the oldest PCM and many studies have been done on them for energy storage. These materials have different melting points with a wide, ranging 15-117 °C [9].

From other features of hydrated salts can be noted to its low price, accessible and inclusive for heat storage applications [10]. Also, these materials have high thermal conductivity and small volume changes during phase changes in comparison to other PCM. Despite advantages, the use of these materials has issues as well. One of the most important problems, which occur in the presence of used metals in thermal energy storage systems, is corrosion. In recent years, many studies have been done on the corrosion behavior of hydrated salts as a group of phase change materials. In a study of the corrosion behavior of hydrated salts in the presence of metals was carried out by Abhat et al [11]. Porosini [12] investigated the corrosion behavior of four widely used hydrate salts that are used as PCM [13-17]. Cabeza et al [17-13] investigated the corrosion behavior of the molten hydrate salts and then they determined corrosion rate of alloys in the presence of salts by immersion tests. Nagano [18] also did research on the corrosion of alloys in the presence of PCM. He evaluated the corrosion behavior of six-alloy in the vicinity of a combination of nitrate and chloride. Romero et al [19] studied the corrosion behavior of four-Aluminum alloy in connection with Glauber salt, and then they published the results of their work. The accumulative roll bonding (ARB) process was invented by Saito et al. [20]. It is one of the severe plastic deformation (SPD) methods to obtain ultrafine grained/nanostructured alloy by applying a very large plastic strain on the material. The various stages of the ARB process have been explained by previous studies [21]. Although, the microstructure and mechanical properties of the ARB aluminum and its alloys have been much studied whereas a little research on the corrosion behavior and properties of fine-grained aluminum alloys produced

by this method have been carried out. In this case, wei et al [22] investigated the corrosion behavior of five-pass ARB aluminum alloys, using electro-chemical polarization in NaCl (3wt%) solution. Shnsi et al [23] studied the corrosion behavior of commercially pure Al and Al-2% Cu alloy, which were under five and six cycles ARB in NaCl (3wt%) solution, respectively. Naeini et al [24] transformed Al 5052 alloy to fine-grained alloy by five cycles ARB and then examined its corrosion behavior in 3.5% wt solution of sodium chloride by immersion test using potasiostate. Almost one of the problems in the ARB process of ARB is pitting corrosion that increases more and more after ARB cycles [23, 24]. It can be found from the literatures that the corrosion behavior of different Al alloys has studied in the 3.5% wt solution of sodium chloride. Since, the behavior of ARB processed alloys in contact with hydrate salts has not been studied as storage of phase change materials yet. Therefore, in the present work, the corrosion behavior of fine-grained AL1100 and the Al6061 alloys by the ARB process, in contact with melted hydrate salts of  $\text{Na}_2\text{HPO}_4 \cdot 12\text{H}_2\text{O}$  and  $\text{Zn}(\text{NO}_3)_2 \cdot 6\text{H}_2\text{O}$  are studied and the results are reported and compared with each other. It can be said that the ARB process may create some metallurgical defects in the microstructure and can change the corrosion behavior of alloys. For example with enhancing the cold work deformation degree, the formation of a passive and protective film is difficult due to the increasing of dislocation density and defects. Thus, the investigation of corrosion behavior of accumulative roll bonding aluminum alloys is needed in contact with melted salts. Therefore, in this research different aluminum alloys produced by ARB were selected and studied their corrosion behavior in contact with melted hydrate salts, which are used as PCMs. The tests used were short term, and the contact time of samples with the molten salts was up to three weeks. This time is enough to evaluation the corrosion rate of aluminum alloys in the molten salts.

## 2. Materials and methodology

Several sheets of Al1100 and Al6061 alloys are used as starting materials. The ARB process is applied on the samples up to 6 cycles in order to obtain ultrafine grained structure. To determine the grain size after ARB process, the electron backscattering diffraction (EBSD) (FE-SEM; Philips XL30) analysis was carried out at 15 KV. In order to study the corrosion behavior of the ARB process, the Na<sub>2</sub>HPO<sub>4</sub>.12H<sub>2</sub>O and Zn (NO<sub>3</sub>)<sub>2</sub>.6H<sub>2</sub>O were purchased from Merck company. Characteristics of the hydrate salts are shown in Table 1. The melting point and pH of PCMs were shown in table 1. . In order to examine, the surface morphology after corrosion testing, an electron microscope (SEM; Philips XL2000) was used at 20 KV. The x-ray diffraction analysis (XRD, PW1719 Philips, X-ray source: Cu-Ka) applied to determine the corrosion products. Furthermore, weight loss of the samples was measured with 0.0001g accuracy. In order to investigate the weight loss of the samples, three periods of time, (6, 12 and 18 days) was considered. After each period, studies were conducted on the samples. In each period, two different environment of the molten hydrate salts (Na<sub>2</sub>HPO<sub>4</sub>.12H<sub>2</sub>O and Zn(NO<sub>3</sub>)<sub>2</sub>.6H<sub>2</sub>O) were selected. Then according to ASTM G1- 0.03 standard [25], the sheets of ABR Al1100 and Al6061 alloys, were cut in the size of 20mm × 10mm × 1mm and were washed with distilled water and acetone, dried and were weighed by a digital scale with 0.0001g accuracy. Then, the samples with the molten PCM were immersed into test tubes under angle of 45°. The test tubes were placed into the thermostatic water bath at 55-60 temperatures range at least 20 °C above the PCM melting temperature. The glass tubes were covered with a plastic film to prevent PCM loss by evaporation to the environment, and PCM degradation. The pH of molten hydrate salts were measured before test and during the period of test every day. After each period of six days, the samples were taken out from the test tubes and degreased with acetone and then cleaned with

70% HNO<sub>3</sub> solution using dipping method to remove the products corrosion and surface deposits

at less than of 10 Sec. Then the samples were cleaned with distilled water and acetone and finally with a digital scale was measured the weight loss of them. To determine the mass change (w) and corrosion rate (CR) were used equation (1), considering the initial m(t<sub>0</sub>) and the weight measured after 6, 12 and 18 days m(t), respectively, [26].

$$CR = \frac{534 w}{D.A.T} \quad (1)$$

In equation (1), the corrosion rate (CR(Mil Penetration Per Year)(mpy)), the mass loss (w(mg)), the density of aluminum alloy D(g/cm<sup>3</sup>) , the metal sample surface area (A(inh<sup>2</sup>)) and the experimental time T(hr) are considered.

### 3. Results and discussion

#### 3.1. The microstructure after ARB process and before corrosion test

Figure 1 shows the EBSD micrograph of ultrafine grain structure of Al 1100 and Al 6061 after 6 cycles ARB process. Low angle grain boundaries (LAGBs) with the angles between 2 to 15 degrees and high angle grain boundaries (HAGBs) with the misorientation above 15 degrees are indicated with red and green lines, respectively. According to Fig. 1 the average grain size of the ARB processed Al 1100 and Al6061 alloys after six cycles is obtained 520nm and 345nm, respectively. This results show the average grain size of the ARB processed Al 1100 is larger than that of the ARB processed Al 6061 alloy at the same cycles. Furthermore, remarkable

reduces are occurred significant in the grain size of the ARB processed Al 1100 and Al6061 alloys processed by 6 cycles. Thus, it can be said that the average grain size is one of the important factors which affect the corrosion behavior of Al alloys.

### **3.2. Study of the corrosion behavior of 6 cycles ARB processed Al1100 and Al6061 alloys, in the molten Na<sub>2</sub>HPO<sub>4</sub>.12H<sub>2</sub>O**

According to Fig. 2, it can be observed for the ARB processed Al1100 and Al6061 alloys in the molten Na<sub>2</sub>HPO<sub>4</sub>.12H<sub>2</sub>O, that the weight loss amounts are 43.33 mg and 50 mg, at the end of 6 days, respectively, while these amounts reaches to 53.33 mg for the Al1100 alloy and 70 mg for the Al6061 alloy at the end of 18 days due to having the larger grain size in the ARB processed Al1100 alloy compared to ARB processed Al6061 alloy. It is clear that the weight loss is high, in both of the specimens after 18 days, although the change rate of weight loss will reduce from 6 to 18 days. The corrosion rate of the samples are shown in Fig. 3. The corrosion rates of ARB processed Al1100 and Al6061 alloys are 192.13 and 220.87 (mill penetration per year) mpy at the end of 6 days, while these data decreases to 78.82 and 103.07mpy after 18 days, respectively. The negative slope of corrosion rate curves, proves these results as well. Because probably an hydroxide layer that can be suggested Al(OH)<sub>3</sub>, which creates on the surface of the Al alloys. As another result, in the molten Na<sub>2</sub>HPO<sub>4</sub>.12H<sub>2</sub>O environment, the ARB processed Al1100 alloy has a lower tendency to corrosion than the ARB processed Al6061 alloy. In other words, after 6 cycles ARB process, the corrosion resistance of the Al1100 alloy is more than Al6061 alloy. Figure 4 shows the results of x-ray diffraction pattern of the ARB Al1100 alloy in the molten

$\text{Na}_2\text{HPO}_4 \cdot 12\text{H}_2\text{O}$  environment. According to Fig. 2, the main corrosion products are  $\text{Al}(\text{OH})_3$  and  $\text{Na}_3\text{Al}(\text{OH})\text{HPO}_4(\text{PO}_4)$ . This analysis confirms the presence of  $\text{Al}(\text{OH})_3$  on the surface of the ARB Al1100 alloy. Brown et al reported that the main reaction between Al1100 alloy, water molecules and oxygen can be happen and then  $\text{Al}(\text{OH})_3$  form [27]. The presence  $\text{Al}(\text{OH})_3$  layer is shown in the XRD pattern, which it can be induced the pitting corrosion. Furthermore, the obtained pH at the end of the 18 days indicates is about 11, which is increased with compared to the pH=10 in the first day. Therefore, the increase of pH is caused  $\text{Al}(\text{OH})_3$  formation. . Figure 5 shows the results of x-ray diffraction pattern for ARB processed Al6061 alloy in the molten  $\text{Na}_2\text{HPO}_4 \cdot 12\text{H}_2\text{O}$  environment. The main products of corrosion are  $\text{Al}_2(\text{PO}_4)(\text{OH})_3$  and  $\text{AlPO}_4 \cdot 2.33\text{H}_2\text{O}$ . This diffraction pattern demonstrates the layer of  $\text{Al}(\text{OH})_3$ , as well. The pH of this environment had a significant increase at the end of 18 days, as reached to 12. According to the Evans theory, if an environment is more alkaline, the corrosion of samples will increase and will form more pits on the surface of ARB processed Al6061 alloy, [26]. Most of the metals that form passive layer in corrosive environments, they are encountered pitting corrosion. Furthermore, reports are indicated that PCM can fail the passive layer and causes to pitting corrosion. [28]. Electron microscopic images at the end of the 18 days (Fig. 6A, B and Fig.8A, B) prove the pitting corrosion of the samples in molten environment. As indicated in Figs. 6 and 7, pits can be seen on the surface with different magnifications for the ARB processed Al1100 and Al6061 alloys in molten  $\text{Na}_2\text{HPO}_4 \cdot 12\text{H}_2\text{O}$  environment A big concentrated hole has been revealed in Fig. 7 as well.

### **3.3. Study of the corrosion Behavior of 6 cycles ARB processed Al1100 and Al6061 alloys, in the molten $\text{Zn}(\text{No}_3)_2 \cdot 6\text{H}_2\text{O}$**

As it shown in Fig. 10, the weight loss data are 50 and 33 mg for the ARB processed Al1100 and Al6061 alloys in the molten  $Zn(NO_3)_2 \cdot 2H_2O$  at the end of 6 days, respectively. These data changes to 60 mg for Al1100 and 46.66 mg for Al6061 at the end of 18 days. The corrosion rate of the samples in terms of mpy has been given in Fig. 11. In both of the alloys, the weight loss after 18 days increases, while the rate of change in weight loss decreases. As the corrosion rate for the ARB processed Al1100 and Al6061 alloys are 221, 69 mpy and 147.24 mpy at the end of 6 days, whereas these data reached to 88, 67 mpy and 68, 71 mpy at the end of the 18 days, respectively.

As a result the corrosion rate declines due to the formation of a protective hydroxide layer on the surface of the alloys. This protective layer appears with white color, which it is probably  $Al(OH)_3$ . Also it can be found that in the molten  $Zn(NO_3)_2 \cdot 2H_2O$  environment similar to  $Na_2HPO_4 \cdot 12H_2O$  environment, the corrosion resistance of the ARB processed Al1100 is more than ARB processed Al6061 alloy. The result of x-ray diffraction pattern of the ARB processed Al1100 alloy in the molten  $Zn(NO_3)_2 \cdot 2H_2O$  environment during 18 days, is observed in Fig. 12. The main corrosion products are  $(Al_2O_3)4 \cdot H_2O$  and  $Al_2(OH)6 \cdot H_2O$  complex consist of a passive oxide layer ( $Al_2O_3$ ) and a hydroxide layer ( $Al_2(OH)_6$ ). The pH at the end of the 18 days is obtained about 4 which has enhanced with compared to the pH of 3 in the first day.

Figure 13 indicates the results of x-ray diffraction pattern for the ARB Al6061 alloy in the molten  $Zn(NO_3)_2 \cdot 2H_2O$  in the 18 days. The original corrosion products in this environment is  $Al_2(OH)6 \cdot H_2O$  complex that both of XRD diffraction show hydroxide layer of  $Al_2(OH)6 \cdot H_2O$  in  $Zn(NO_3)_2 \cdot 2H_2O$ . The pH of the environment after 18 days, reached to 4, as well.

Since, the corrosion products of ARB processed Al6061 alloy is less than the corrosion products of ARB processed Al1100 alloy in the molten  $Zn(NO_3)_2 \cdot 2H_2O$  ARB processed Al1100. It seems that the passive layer formation on the surface of the ARB processed Al6061 alloy could

completely cover the surface, while for the ARB Al1100 alloy, it couldn't cover whole of the surface. Of course, the similar results have been obtained from the x-ray diffraction pattern of ARB processed Al1100 and Al6061 in the molten  $\text{Na}_2\text{HPO}_4 \cdot 12\text{H}_2\text{O}$  before, as well. So that the found complex in the corrosion products of the ARB processed Al6061 in the molten  $\text{Na}_2\text{HPO}_4 \cdot 12\text{H}_2\text{O}$  unable to play as a protective layer. The SEM images for ARB processed Al1100 and Al6061 alloys in molten  $\text{Zn}(\text{NO}_3)_2 \cdot 2.6\text{H}_2\text{O}$  during 18 days, have been given in Fig. 14 and 15, respectively.

In the ARB processed Al1100 sample in the  $\text{Zn}(\text{NO}_3)_2$  environment, small pits have been appeared. According to the Fig.15, the appearance of the pits is different on the surface of the ARB processed Al1100 in the molten  $\text{Na}_2\text{HPO}_4 \cdot 12\text{H}_2\text{O}$ . Thus, the less damage has happened on the surface of Al1100 sample in the  $\text{Zn}(\text{NO}_3)_2 \cdot 2.6\text{H}_2\text{O}$  environment than  $\text{Na}_2\text{HPO}_4 \cdot 12\text{H}_2\text{O}$  environment. The important approach is that any evidence of pit as a pitting corrosion was found on the surface of the ARB Al6061 in the molten  $\text{Zn}(\text{NO}_3)_2 \cdot 2.6\text{H}_2\text{O}$ . It seems that the number of the pits is directly related to formed protective layer on the surface of the samples in corrosive environments. The results of XRD and SEM in this study revealed that the formation of the protective layer with complex composition on the alloy surface in a corrosive environment increases weight loss due to the uniform corrosion and the number of pits due to pitting corrosion. However, when the protective layer has a simple composition, corrosion rate of sample will reduce. Presumably, complex compounds cannot completely cover the surface continuously to act as a protective layer. Furthermore, the formation of  $\text{Al(OH)}_3$  layer on the surface of samples leads to pitting corrosion on the surface of samples [27].

#### 4. Discussion

The presence of oxygen in the upper zone of the tube test, in comparison with the low oxygen content available in the molten phase change materials can play as a concentration cell. The formation of  $\text{Al(OH)}_3$  (see fig. 4, and 5), on the surface of the ARB processed Al1100 and Al6061 alloys shows a corrosion mechanism due to differential oxygen concentration, which induces the low oxygen content zone become cathodic with respect to the high oxygen content zone. The observation of  $\text{Al(OH)}_3$  in the corrosion product is shown that the corrosion mechanism of the ARB processed Al1100 and Al6061 alloys is related to watery systems, which the Al surrounding impurities becomes anodic to these impurities, and then they are dissolved into the solution. The formation of  $\text{Al(OH)}_3$  is confirmed the  $\text{Al}^{3+}$  cation, and dissolution of Al alloys with contact phase change materials. Furthermore, the presence of  $\text{Al}_2(\text{PO}_4)(\text{OH})_3$  and  $\text{AlPO}_4 \cdot 2.33\text{H}_2\text{O}$  in the corrosion products show the degradation of the PCM (see Fig. 4, and 5). However, the oxide that usually forms in the corrosion of the ARB processed Al1100 and Al6061 alloys is a dense thin alumina layer, which can be created the pitting corrosion phenomena. However, the oxide that usually forms in the corrosion of the ARB processed Al1100 and Al6061 alloys is a dense thin alumina layer, which can be created the pitting corrosion phenomena (see Fig. 6, 8, 14 and 15) due to failure, flaw formation and localize defects to according Evans theory. From Fig. 6, 8, 14 and 15, it can be observed the specimens of the ARB processed Al1100 and Al6061 alloys are corroded in contact with phase change materials with different corrosion rate due to having different microstructure. This behavior is confirmed the corrosion mechanism observed in the specimens, due to different oxygen concentration, which is fully immersed in PCMs or partially in contact with air. the ARB processed Al1100 and Al6061 alloys in contact with phase change materials, tend to severe pitting corrosion, and also degradation of the PCM occurs due to the formation of alkaline compound.

It was known that the grain boundaries have an important role in properties of ultrafine grain structure. Furthermore, in polycrystalline structure the corrosion phenomena are severely related to interfaces, and are susceptive to the grain boundary structure. Because, grain boundaries are more active sites than grains and are preferential sites for corrosion initiation. Usually, the corrosion resistance of grain boundary in molten salts is depended to the internal energies of them. Therefore, it seems the increase in the internal energy makes enhance in the corrosion rate of samples in the molten salts. The ARB process induces to creating ultrafine grained with high ratio of nonequilibrium grain boundaries and internal energy. In addition, close to grain boundaries and inside of grains, the density of dislocation, residual stress, and other metallurgical defects are extremely high. Thus, the presence of these factors causes more regions to corrosion initiation, and then decreases the corrosion resistance. Another effect of ultrafine grained microstructures is the suitable surface ratio of anode to cathode on the corrosion rate of alloys. As a result, high corrosion rate is related to the larger surface ratio of the anodes (grain boundaries) to the cathode (grains). The grain boundaries are active regions, while the number of the ARB cycle is enough, and ultrafine grained microstructures is provided. Therefore, there is significant difference between the grain boundaries (large anodic) and the grains (small cathode), and the corrosion tendency is high.

## 5. Conclusions

Short-term corrosion tests for two the six cycles ARB processed Al1100 and Al6061 alloys in two different hydrate salts were conducted during the 18 days. Based on the results of the experiments, the corrosion rate of the ARB processed Al 6061 alloy in the molten

$\text{Na}_2\text{HPO}_4 \cdot 12\text{H}_2\text{O}$  is greater than ARB processed Al1100 alloy. The formed pits with the pitting corrosion tendency in ARB processed Al6061 alloy are larger than the pits on the surface of the ARB processed Al1100. In another word, the corrosion resistance of the ARB processed Al1100 alloy is more than ARB processed Al6061 in the molten  $\text{Na}_2\text{HPO}_4 \cdot 12\text{H}_2\text{O}$  environment. However, the results in the molten  $\text{Zn}(\text{NO}_3)_2 \cdot 6\text{H}_2\text{O}$  is different. Thus, the rate of corrosion of the ARB processed Al6061 alloy is less than ARB processed Al1100 alloy in the mentioned environment. Furthermore, the resistance to the formation of pits on the surface of Al6061 alloy is much more than Al1100 alloy in the same environment. Thus, pits were observed on the surface of the ARB processed Al6061 alloy in the molten  $\text{Zn}(\text{NO}_3)_2 \cdot 6\text{H}_2\text{O}$  during the 18 days. It is due to the formation of an appropriate protective layer on the surface of the Al6061 alloy. From the results, it seems that the presence of complex compounds in corrosive environments on the surface of alloys, causes to destroy the uniform protective coating and accelerate its corrosion rate. The weight loss diagram, corrosion rate, XRD analysis and SEM pictures from the surface of samples confirm this case, after 18 days of immersion in the molten  $\text{Zn}(\text{NO}_3)_2 \cdot 6\text{H}_2\text{O}$ . According to figures and diagrams can be understood that the corrosion rate slightly enhances with applying the ARB process. As a final result, severe plastic strain, an increase of dislocation Density, fine-grained alloy and increasing of the surface of alloy by the ARB process, caused to reduce the corrosion resistance of the ARB alloys. Because, in ultrafine grained microstructures, the grain boundaries are the more active sites than the grains, it causes to enhance the corrosion rate of specimens prepared by 6 cycles in contact with molten salts.

## 5. Acknowledgments

Authors gratefully thank Semnan University for partially supporting the research.

**6. References**

- [1] B. Zalba, J.M. Marin, L.F. Cabeza, H. Mehling, Review on thermal energy storage with phase change: materials, heat transfer analysis and applications, *Appl. Therm. Eng.* 23 (2003) 251–283.
- [2] M.M. Farid, A.M. Khudhair, S.A. Razack, S. Al-Hallaj, A review on phase change energy storage: materials and applications, *Energy Conversion and Management* 45 (2004) 1597–1615
- [3] X. Wang, E. Lu, W. Lin, T. Liu, Z. Shi, R. Tang, C. Wang, 2000. Heat storage performance of the binary systems neopentyl glycol/pentaerythritol and neopentyl glycol/trihydroxy methylaminomethane as solid phase change materials, *Energy Conservation and Management* 41(2000) 129-134
- [4] P.C. Eames, P.W. Griffiths: Thermal behavior of integrated solar collector/storageunit with 65C phase change material. *Energy Conversion and Management* 47 (2006) 3611–3618
- [5] A. Ku̇rklu, A. Ȯzmerzi, S. Bilgin: Thermal performance of a water-phase change material solar collector. *Renewable Energy* 26 (2002) 391–399
- [6] E. Oró, A. Gil, L. Miró, G. Peiró, S. Álvarez, L.F. Cabeza: Thermal energy storage implementation using phase change materials for solar cooling and refrigeration applications. *Energy Procedia* 30 (2012) 947 – 956
- [7] P.H. Biwole, P. Eclache, F. Kuznik, Phase-change materials to improve solar panel's performance. *Energy and Buildings* 62 (2013) 59–67
- [8] E.M. Alawadhi, Using phase change materials in window shutter to reduce the solar heat gain. *Energy and Buildings* 47 (2012) 421–429.
- [9] G. Lane, Latent heat materials, CRC Press 1, Boca Raton, Florida. 1983
- [10] G.A Lane, Macro-encapsulation of PCM, Report No. oro/5117-8, Dow Chemical Company, Midland, Michigan (1978) 152
- [11] A. Abhat, Low temperature latent heat thermal energy storage: heat storage materials, *Solar Energy* 30 (1983) 313-331
- [12] F.C. Porisini, Salt hydrates used for latent heat storage: corrosion of metals and reliability of thermal performance, *Solar Energy* 41 (1988) 193–197
- [13] L.F. Cabeza, J. Illa, J. Roca, F. Badia, H. Mehling, S. Hiebler, F. Ziegler, Immersion corrosion tests on metal-salhydrate pairs used for latent heat storage in the 32 to 36C temperature range, *Mater. and Corros.* 52 (2001) 140–146.
- [14] L.F. Cabeza, J. Illa, J. Roca, F. Badia, H. Mehling, S. Hiebler, F. Ziegler, Middle term immersion corrosion testson metal-salt hydrate pairs used for latent heat storage in the 32 to 36C temperature range, *Mater. And Corros.* 52 (2001) 748–754.

[15] L.F. Cabeza, F. Badia, J. Illa, J. Roca, H. Mehling, F. Ziegler, Corrosion experiments on salthydrates used as phase change materials in cold storage, IEA ECES IA Annex 17 Kick-off Workshop, Lleida (Spain), 2001.

[16] L.F. Cabeza, H. Mehling, S. Hiebler, Immersion corrosion tests on metal-salt hydrate pairs used for latent heatstorage in the 48 to 58C temperature range, Mater. and Corros., in press

[17] L.F. Cabeza, J. Roca, M. Nogueés, H. Mehling, S. Hiebler, Long term immersioncorrosion tests on metal-PCM pairs used for latent heat storage in the 24 to 29DegC temperature range, Mater. And Corros. 56 (2005) 33–38

[18] K. Nagano, K. Ogawa, T. Mochida, K. Hayashi, H. Ogoshi, Performance of heatcharge/discharge of magnesium nitrate hexahydrate and magnesium chloridehexahydrate mixture to a single vertical tube for a latent heat storage system, Appl. Therm. Eng. 24 (2004) 209–220

[19] A. García-Romero, A. Delgad, A. Urresti, K. Martín, J.M. Salap: Corrosion behavior of several aluminium alloys in contact with a thermalstorage phase change material based on Glauber's salt, Corros. Scie. 51 (2009) 1263–1272

[20] Y. Saito, H. Utsunomya, N. Tsuji, T. Sakal, Novel ultra-high straining process for bulk Materials development of the accumulative roll-bonding (ARB) process, Acta mater. 47 (1999) 579-583

[21] E. Borhani, H. Jafarian, Effect of pre-existing nano sized precipitate on microstructure and mechanical property of Al-0.2wt% Sc Highly deformed by ARB Process, J. of ultraf. grained and nanostruc. Mater. 47 (2014) 1-7

[22] W. Wei, K.X. Wei, Q.B. Bo du, Corrosion and tensile behaviors of ultra-fine grained Al–Mn alloy produced by accumulative roll bonding" Mater. Sci. and Eng. A (2007) 536–541.

[23] F. Shhnji., I. Taku, T. Nobohiro, M. Yoritoshi, Corrosion behavior of ultra fine grained Al and Al- 2% Cu alloy by ARB process " Materials *Corrosion and Protection of Light Metal Alloys: Proceedings of the International Symposium*. Vol. 2003. The Electrochemical Society, 2004.

[24] Mehdi Fadaei Naeini, M.H.S., Hassan Fattahi , Mehdi EizadjouMehdi Fadaei Naeini,Mohammad Hossain Shariat, Hassan Fattahi , Mehdi Eizadjou, Pitting corrosion of nanostructure AA5052 aluminum alloy fabricated by Accumulative Roll-Bonding in chloride media. Journal of Advanced Materials and Technologies, 2009. 2(1): p. 75-85.

[25] Anon, Standard Practice for Preparing, Cleaning, and Evaluating Corrosion Test Specimens, Annual Book of ASTM Standards, Section 3, Metals Test Methods and Analytical Procedures 3 (1996), American Society for Testing and Materials (ASTM) West Conshohocken, PA, USA,

[26] M.G. Fontana, Corrosion Engineering(Third Edition), McGraw-Hill, 1987.

[27] R.H. Brown, R.B. Mears, The electrochemistry of corrosion, Transac. of the Electrochem. Soci. 74 (1938) 495.

[28] GA Lane—Solar heat storage latent heat material. Vol II.—CRCPress. Inc—1986

[29] F. Lockwood, S. Lee, J. Faunce and J.A.S. Green, “Pitting Corrosion of Aluminium Alloy”, Application of Surface, 20 (1985) 339-346.

Table 1. Characteristics of the hydrate salts

Hydrate salts	T <sub>M</sub>	pH
Na <sub>2</sub> HPO <sub>4</sub> .12H <sub>2</sub> O	35°C	10
Zn(NO <sub>3</sub> ) <sub>2</sub> .6H <sub>2</sub> O	36°C	3

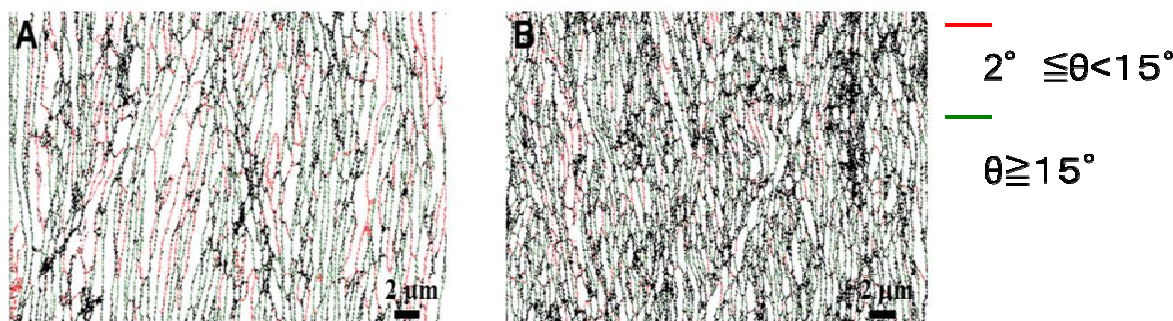
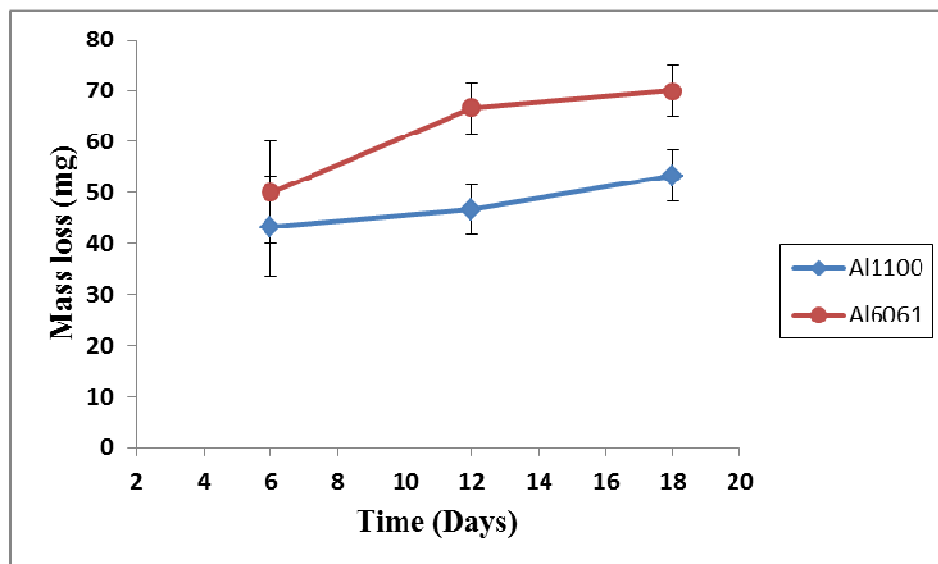


Figure 1. The EBSD micrograph of the six cycles ARB processed alloys A) Al1100, (B Al6061

Fig2. The weight loss of sampels in the molten Na<sub>2</sub>HPO<sub>4</sub>.12H<sub>2</sub>O

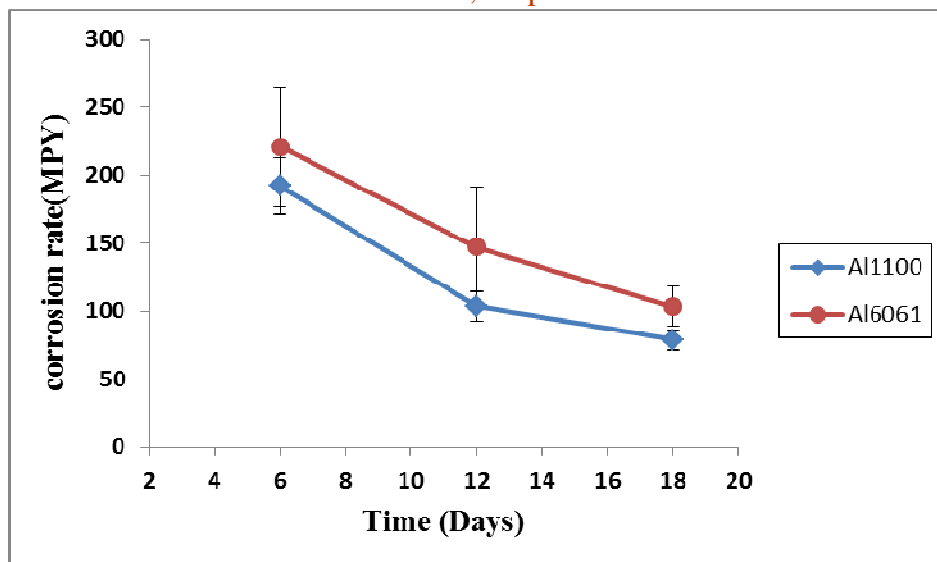
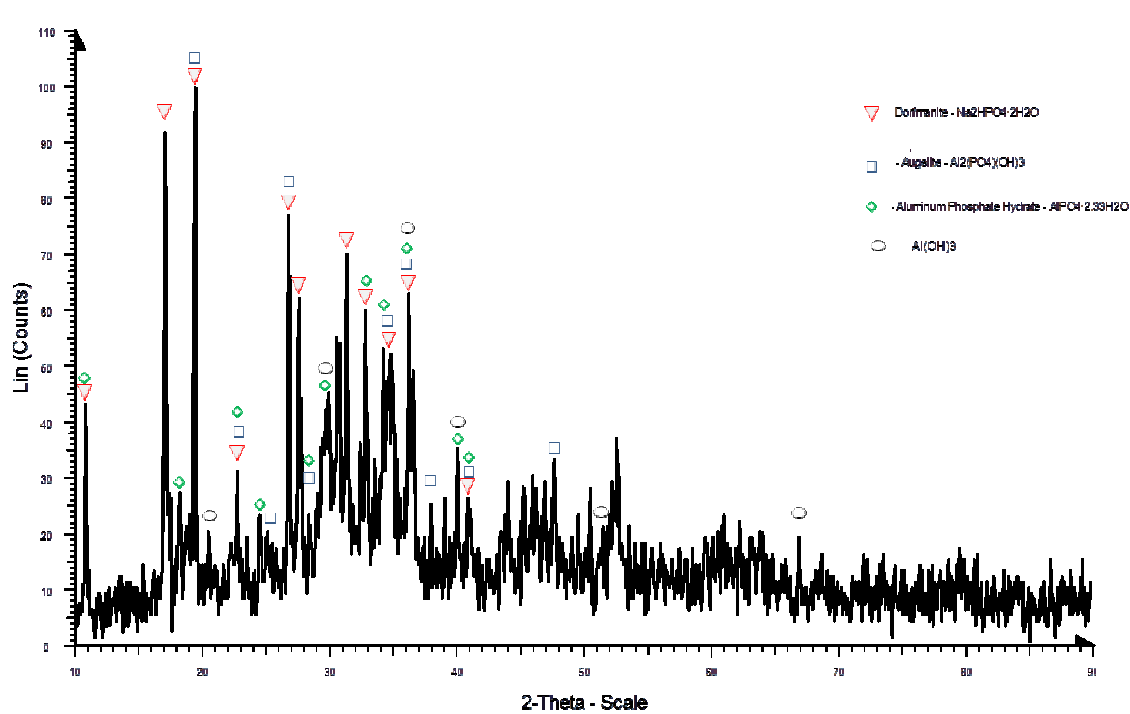
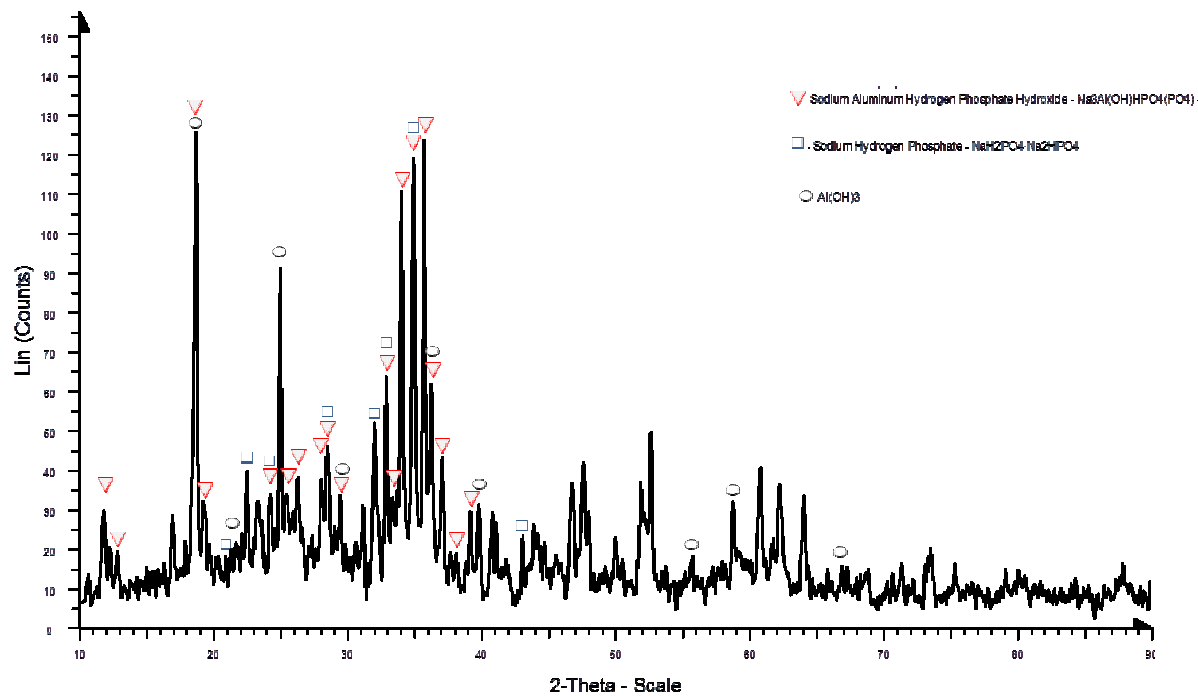


Fig 3. The corrosion rate of the samples in the molten Na<sub>2</sub>HPO<sub>4</sub>.12H<sub>2</sub>O



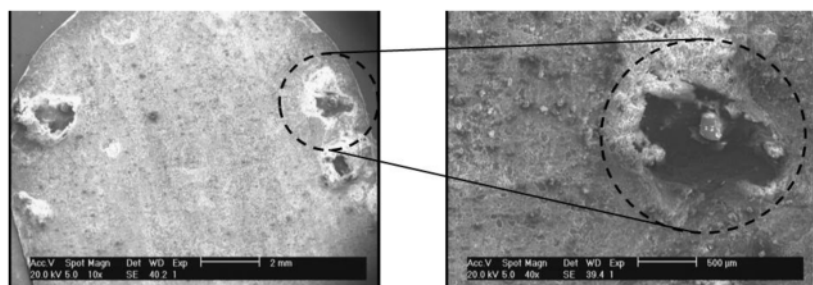


Fig.6. The SEM images for ARB Al1100 alloy, in the molten  $\text{Na}_2\text{HPO}_4 \cdot 12\text{H}_2\text{O}$ ,  
A) magnification of 10x, B) magnification of 40x.

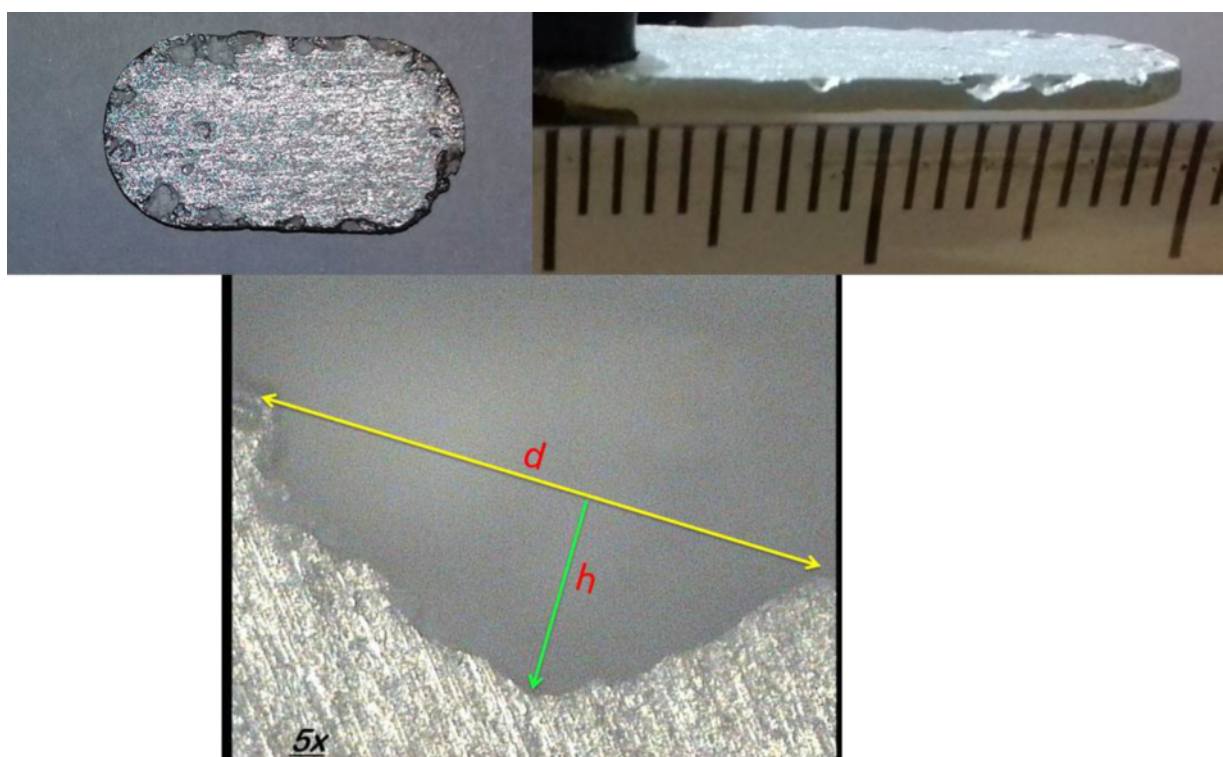


Fig. 7. Macrograph of ARB aluminium alloy 1100 specimens tested for 18 days, at 50 °C, fully immersed in the molten  $\text{Na}_2\text{HPO}_4 \cdot 12\text{H}_2\text{O}$ .

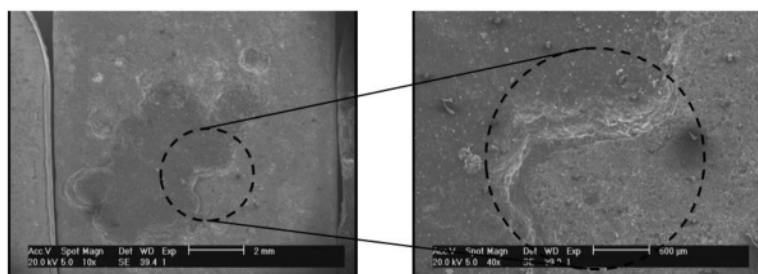


Fig 8. The SEM images for ARB Al6061 alloy, in the molten  $\text{Na}_2\text{HPO}_4 \cdot 12\text{H}_2\text{O}$   
(A magnification of 10x, (B magnification of 40x)

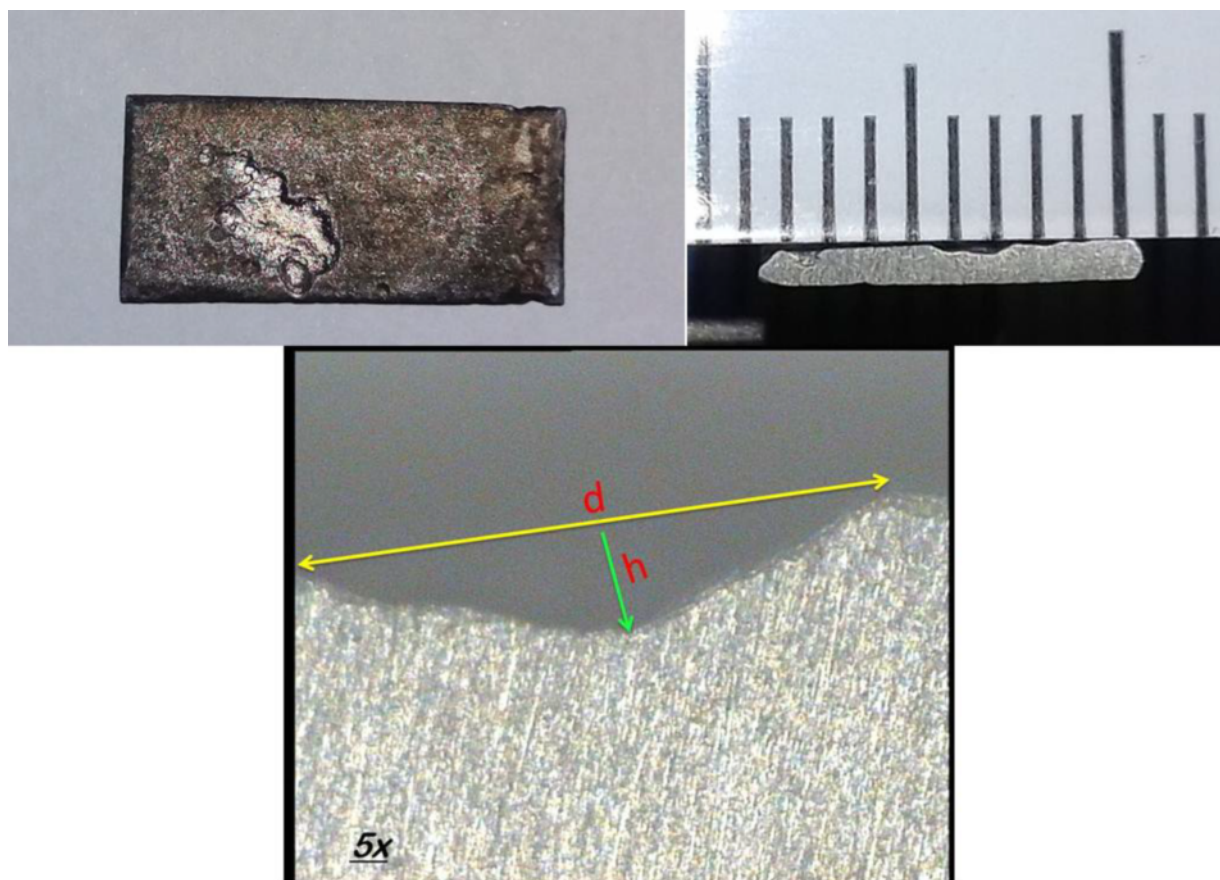
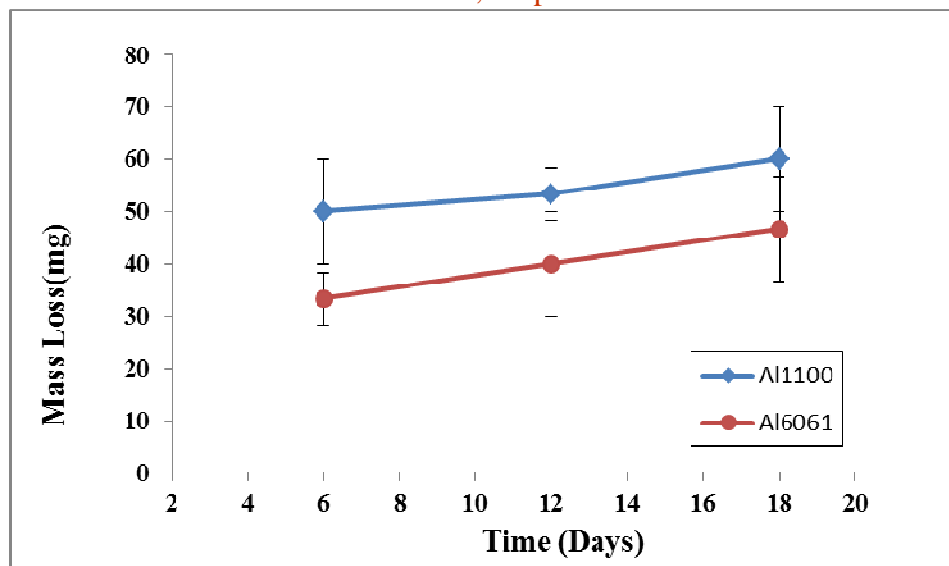
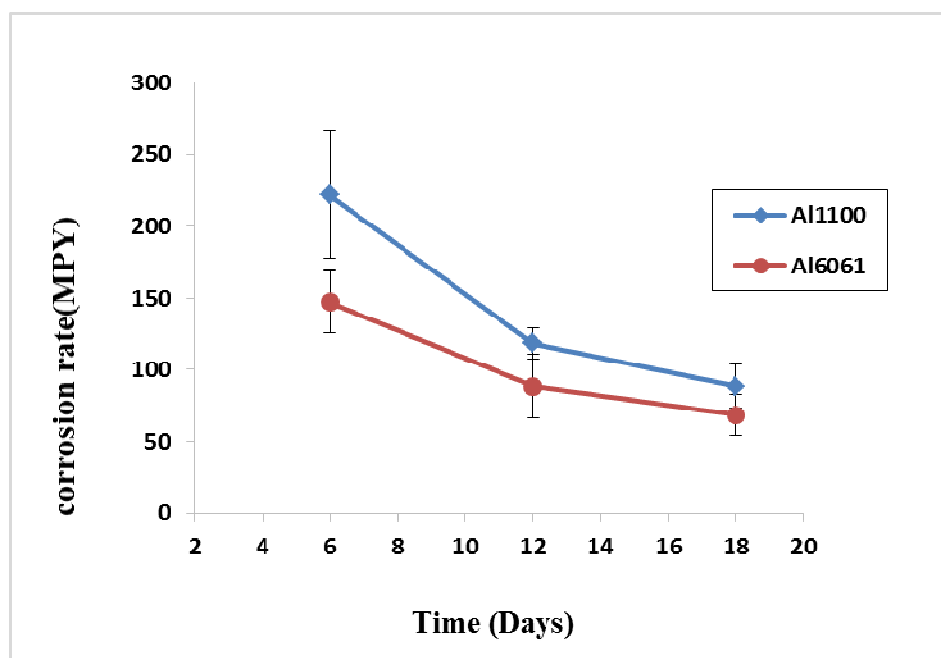


Fig. 9. Macrograph of ARB aluminium alloy 6061 specimens tested for 18 days, at 50 °C, fully immersed in the molten  $\text{Na}_2\text{HPO}_4 \cdot 12\text{H}_2\text{O}$ .

Fig. 10. The weight loss curve of sampels in the molten  $\text{Zn}(\text{NO}_3)_2 \cdot 6\text{H}_2\text{O}$ Fig 11. The corrosion rate curve of the samples in the molten  $\text{Zn}(\text{NO}_3)_2 \cdot 6\text{H}_2\text{O}$

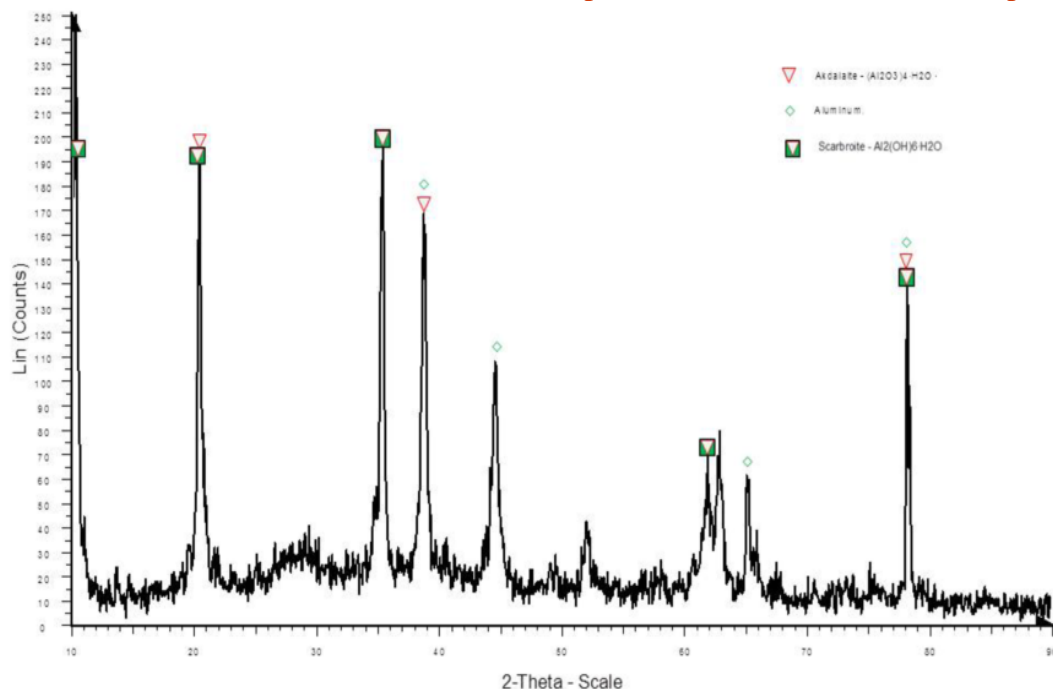


Fig 12. X-ray diffraction pattern of the ARB Al1100 alloy in the molten  $Zn(NO_3)_2 \cdot 6H_2O$ .

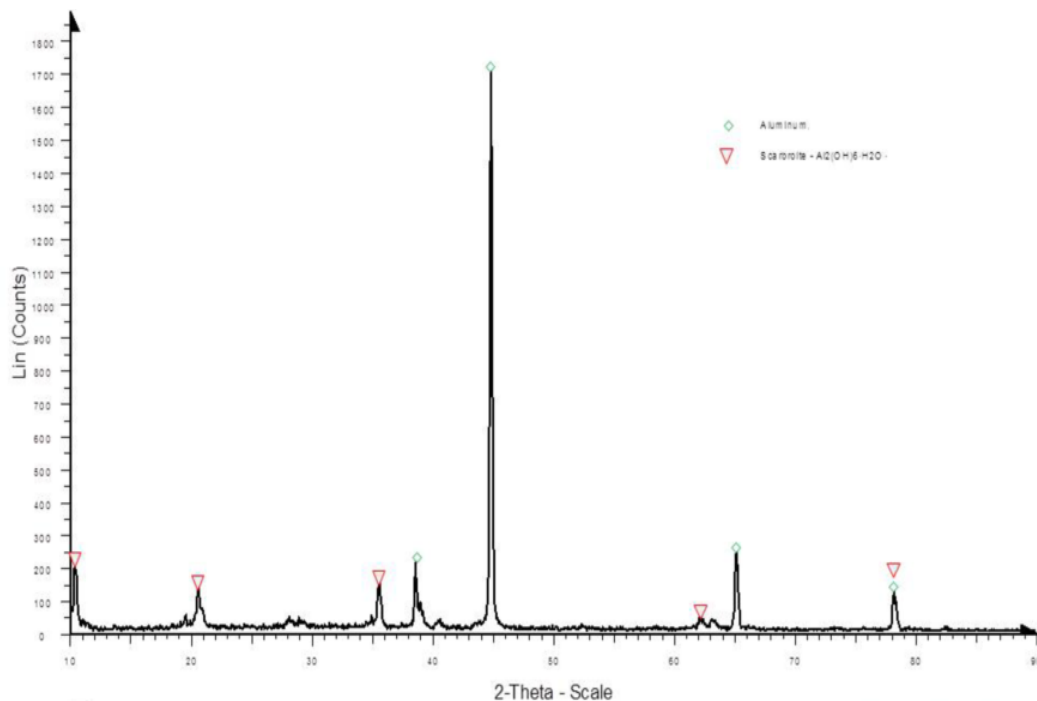


Fig 13. The results of X-ray diffraction pattern for ARB Al6061 alloy in the molten  $Zn(NO_3)_2 \cdot 6H_2O$

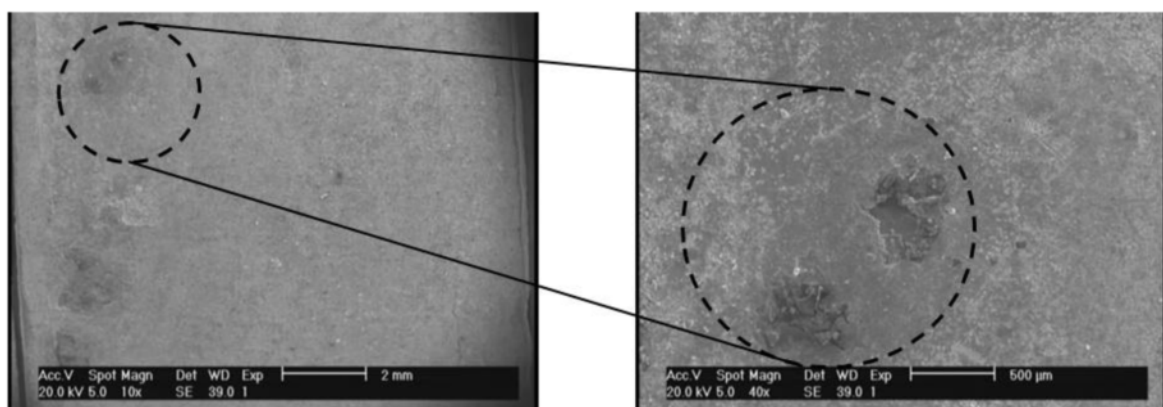


Fig14. The SEM images for ARB Al1100 alloy, in the molten  $Zn\ (NO_3)_2 \cdot 6H_2O$ ,  
A) Magnification of 10x, B) Magnification of 40x.

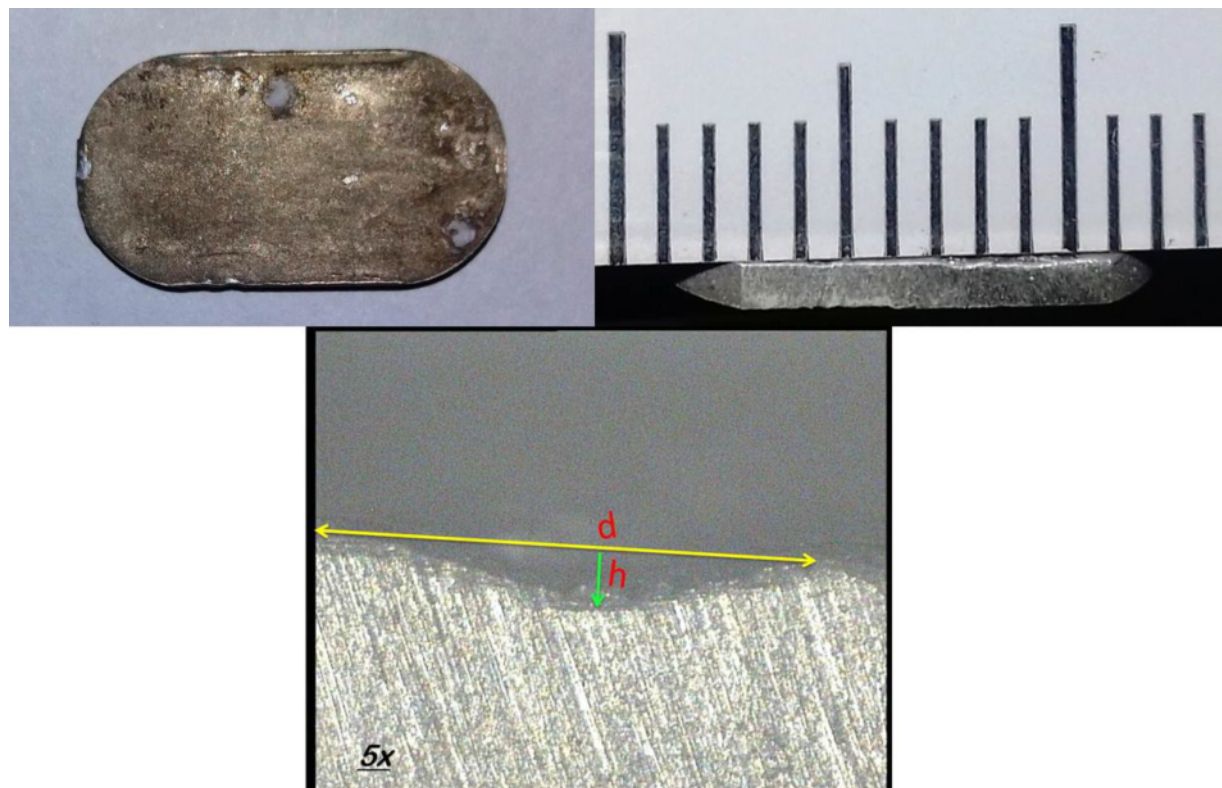


Fig.15. Macrograph of aluminium alloy 6061 specimens tested for 18 days, at 50 °C, fully immersed in the molten  $Zn\ (NO_3)_2 \cdot 6H_2O$ .

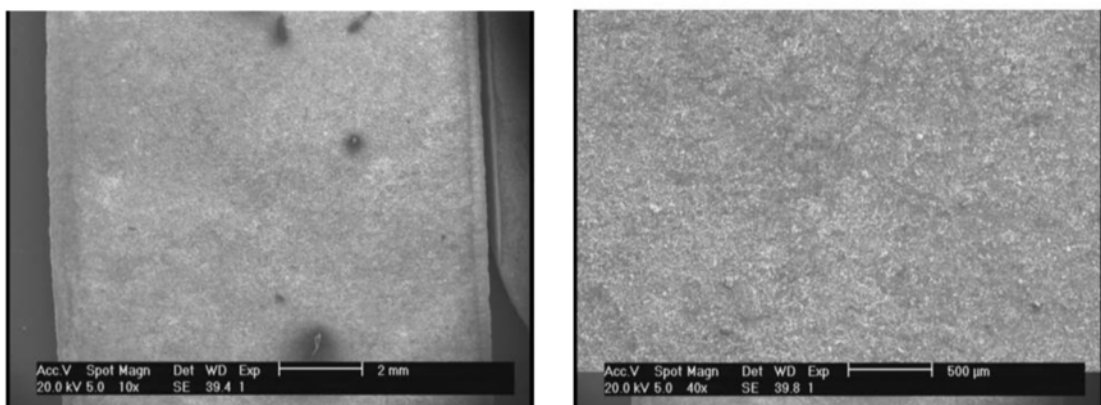


Fig16. The SEM images for ARB Al6061 alloy, in the molten  $Zn(NO_3)_2 \cdot 6H_2O$ ,

A) Magnification of 10x, B) Magnification of 40x.